J. Appl. Comput. Mech., xx(x) (2026) 1-14
DOI: 10.22055/jacm.2026.48857.5554
ISSN: 2383-4536
jacm.scu.ac.ir

Shahid Chamran University of Ahvaz

Journal of Applied and Computational Mechanics

Research Paper

Experimental and Modeling Approach to Investigate the Influence of Temperature on Surge and Swab Pressures in Water-Based Drilling Muds

Mohsen Mombeini, Mohammad Torkaman, Milad Mohammareh Nezhad Rabieh, Morteza Moradi

Department of Chemical Engineering, Faculty of Engineering, Shahid Chamran University of Ahvaz, Ahvaz, Iran

Received October 24 2025; Revised May 28 2026; Accepted for publication May 29 2026.
✉ Corresponding author: M. Torkaman (m.torkaman@scu.ac.ir)

Abstract. One of the major concerns of drilling a high-temperature well is the problem of surge and swab pressures that are highly affected by temperature changes. Still, there has been no comprehensive try to investigate the effect of temperature on these phenomena. So, in this study, a set-up device is designed and built to measure the surge and swab pressures at different conditions. The experimental results indicate that a temperature increment from 25 to 85°C could cause a decline in surge and swab pressures by 2.8 and 2.86% respectively. Also, the findings reveal that increasing the pipe diameter has a greater impact on increasing the intensity of these phenomena than elevating the pipe tripping speed. In the next step, a mathematical model is used to scrutinize the action mechanisms of different parameters and also to find the governing factors on surge and swab pressures. The modeling outputs show a validation of 97% with experimental results. Also, the modeling indicates that an increment in pipe diameter and tripping speed cause higher turbulence of the flow thus leading to more inaccuracy of the model predictions (up to 94% validation for higher tripping speeds and 90% for larger pipe diameters).

Keywords: Accumulative pressure, Surge pressure, Swab pressure, Tripping operation, Modeling.

1. Introduction

Today due to the vast extraction from oil reservoirs and considering the fact that most of them are in their mature stage, the oil is produced from deeper reservoirs that are in high-pressure and high-temperature (HPHT) conditions [1]. As the time to reach these depths is so long, reducing the operation time and especially the dead time is considered as a major concern. One of the most time-consuming stages of the drilling operation is pipe tripping that can be controlled by bottom-hole pressures (BHPs). Two of these BHPs are surge and swab that occur during pipe-out and pipe-in operations respectively. These pressures can be affected by different competitive parameters such as drilling fluid plastic viscosity, yield point, gel strength, diameter ratio (pipe diameter/hole diameter), pipe velocity, drill string concentricity, and wellbore geometrical shape [2]. Other parameters such as pipe roughness and formation elasticity apply less effect on these phenomena [3]. Recognizing these parameters and their effect may bring further improvement in drilling operation optimization and thus many investigations have been executed in this field.

To investigate the effective parameters on surge and swab pressures, Crespo et al. constructed a set-up device based on a narrow-slot model that its results were acceptable for diameter ratios of more than 0.4. Their findings showed that the eccentricity of the drill string could reduce the amount of surge and swab pressures by up to 45% [4]. Also, they found that an increment in drilling fluid yield point, could reduce the impact of pipe velocity by 66% [2] in agreement with results obtained by other research [5, 6]. The surge and swab phenomena in horizontal and inclined wells were investigated by Srivastav et al. and their findings stated that considering the drill string in a concentric position would lead the predictions to overestimate the surge and swab pressures. They also suggested a correction coefficient depended on wellbore geometry and drill string concentricity that could improve the model validation to 87% [5]. Studying the impact of diameter ratio on surge and swab pressures via modeling by Mme and Skalle demonstrated that an increase in wellbore diameter allows the fluid to flow at higher velocities and thus reduces the surge and swab pressures [6] that is also seen by Al-Abduljabbar et al. [7]. They also concluded that the only controllable parameter during drilling operation is pipe tripping velocity and parameters such as drilling fluid viscosity and yield point are strictly restricted by drilling operation conditions and could not be regulated manually [3]. Tang et al. studied the influence of rheological properties of drilling fluids on surge and swab pressures and depicted plastic viscosity as the most effective parameter that if regulated accurately, the surge and swab pressures could be reduced in advance [6] as it is also found by He et al. [8].

Among the various influencing parameters, temperature plays a particularly important role because it simultaneously affects both the rheological behavior and density characteristics of drilling fluids. Temperature significantly affects surge and swab pressures because it directly alters the rheological and physical properties of drilling fluids during tripping operations. Increasing temperature reduces drilling fluid viscosity, yield point, and gel strength, thereby lowering annular flow resistance and weakening

Published online: July 23 2026

the piston-like pressure generation mechanism around the moving drill string. Simultaneously, temperature-induced density reduction affects hydrostatic pressure, leading to variations in the bottom-hole pressure profile. Under HPHT conditions, these coupled rheological and density changes become more pronounced and may substantially influence pressure fluctuations, equivalent circulating density, and wellbore stability. Therefore, accurate evaluation of temperature-dependent drilling fluid behavior is essential for reliable prediction and control of surge and swab pressures during drilling operations [6, 8-10].

One of the other effective parameters on surge and swab pressures is the gel strength of drilling fluid that is a result of different polymers existing in the fluid like xanthan gum (XG) and polyacrylamide (PAM). Krishna et al. realized increasing the concentration of these polymers would lead to higher gel strength of drilling fluids and consequently, the surge and swab pressures could be escalated up to 18% [11-13]. Another impressive factor in surge and swab pressures is whether to use a close-ended pipe or an open-ended one. Modeling this state by He et al. with 95% validation to experimental results, revealed that a close-ended pipe could increase the accumulative pressure by 40% confining the pipe-tripping velocity margins even more [8, 14]. The investigation of Al-Abduljabbar et al. on surge and swab pressures showed that a change of 1 inch in pipe diameter could make a change of 75% in these phenomena while changing the string length by even 100 ft applies no drastic impact on them [7]. Tang et al. modeled the annulus as an elliptic-shaped pipe for the first time and the outcomes indicated that increasing pipe eccentricity from 0 to 50% could reduce the accumulative pressure while eccentricities more than 50% would make an incline in the slope. The modeling predictions showed a validation of 95% of the experimental results [15]. Different salts and their concentration in drilling fluids could also sequel in surge and swab pressure changes. Mohammad and Belayneh developed a simplified analytical model to predict surge and swab pressures in eccentric and concentric annuli using power-law and modified yield-power-law fluid rheological models. Their model incorporated tripping speed, eccentricity, and fluid parameters and was validated against experimental data with less than 10% average error. The study demonstrated that physics-based rheological models can accurately describe drilling fluid behavior, emphasizing the need for calibration and potential integration with machine learning for improved prediction accuracy [16]. The study on surge and swab pressures modeling using physics-based simulations and machine learning techniques was conducted by Mohammad et al. They compared several rheological models and observed inconsistencies among physics-based predictions, emphasizing the need for proper calibration. The researchers showed that machine learning models such as Artificial Neural Network (ANN) and Long Short-Term Memory (LSTM) achieved higher accuracy, proving their effectiveness for real-time drilling optimization and intelligent well planning [17]. The review on surge and swab pressure prediction in the oil and gas industry was conducted by Yusuf et al. The study highlighted that fluid rheology, tripping speed, wellbore eccentricity, and diameter ratio significantly influence surge/swab pressures, with increases in rheological parameters leading to higher pressure gradients (up to ~18% for gel strength). It emphasized the need for simplified analytical models and robust experimental data to improve prediction accuracy and reduce Non-Productive Time (NPT) during drilling operations [18]. Zhang et al. conducted this study to improve the prediction of transient surge and swab pressures during tripping in narrow pressure windows. Using the Herschel–Bulkley model, which better represents drilling fluid behavior, the study showed that oil-based and polymer muds reduce pressure compared to water-based muds. It also found that increasing tripping speed, rheological parameters, and pump rate raises surge–swab pressure, emphasizing the need for strict control to ensure safe and efficient drilling [19]. Salih and Hadi analyzed surge and swab pressures during tripping operations in the Rumaila oilfield to determine optimal pipe movement speeds and minimize drilling problems. Using a dynamic surge–swab model and field case studies, they found that tripping speed, annular clearance, and Bottom Hole Assembly (BHA) design have the greatest impact on pressure fluctuations. Their results showed that maintaining tripping speeds between 80–90 ft/min prevents surge and swab pressures from exceeding formation fracture limits, thus improving drilling efficiency and reducing non-productive time [20]. Lenwoue et al. studied the impact of swab and surge pressure on time-dependent wellbore fracture development. Their findings showed that swab and surge pressures increased fracture width by up to 69.92% near the wellbore and narrowed the safe mud window over time, with collapse pressure rising 14.33% and fracture pressure decreasing 13.80%. The researchers demonstrated that numerical modeling can accurately predict natural fracture growth and optimize wellbore reinforcement to mitigate lost circulation during drilling operations [21]. Wei et al. [22] developed a full-scale BHA fluid–structure interaction model to study bottom-hole pressure fluctuations during tripping operations. Their findings showed that tripping speed was the dominant factor, with surge pressure increasing from 1.597 to 2.627 MPa as speed rises from 0.2 to 0.8 m/s, while swab pressure increases by 0.138 MPa. Increasing drilling fluid viscosity from 2 to 10 mPa.s raises surge pressure by 278.7%, and density from 1.4 to 2.0 gr/cm^3 increases it by 75.5%. Wang et al. [9] proposed a predictive model for surge pressure estimation in HPHT wells by incorporating temperature- and pressure-dependent drilling fluid rheology. The model considered open-ended pipe and closed-ended pipe configurations and evaluates yield stress, annular ratio, and tripping speed effects. Results showed tripping speed as the dominant factor, while annular ratios below 0.55 or above 0.65 lead to blockage behavior in open-ended pipe systems, with 0.65 to 0.75 identified as a critical range. Li et al. [10] developed a high-fidelity transient pressure model for Managed Pressure Drilling (MPD) in HPHT wells, incorporating choke settings, fluid properties, and drill string eccentricity. The model was validated with field data, showing less than 5% error in peak surge pressure. Their findings indicated that choke opening, HPHT conditions, and eccentricity significantly influence surge and swab behavior, affecting pressure wave propagation and secondary swab effects.

It can be said that although many investigations have been done on surge and swab pressures, still no experimental or modeling results reported the effect of temperature changes on these phenomena comprehensively. In this study, a set-up device was designed and built to stimulate the pipe-tripping operation. The device was equipped with pressure gauges alongside thermometers so the influence of the temperature changes on surge and swab pressures could be observed. Also, the impact of two controllable parameters of pipe velocity and diameter ratio was studied to further investigate the effect of temperature changes at different conditions. To find the exact reason for pressure changes due to surge and swab pressures at different conditions, a mathematical model was used and it provided the ability to predict the surge and swab pressure changes where the set-up device was not able due to the limitations of the device.

2. Experimental Section

2.1. Test conditions

To make the experimental condition similar to the real bottom-hole condition, the tests were conducted in a wide range of temperatures (25, 45, 65, and 85°C). Also, to investigate the impact of pipe diameter and drill string tripping velocity on surge and swab pressures, two different pipes with diameters of 1.5 and 1.75 inch ran into the borehole with speeds of 1 and 1.5 ft/s.

2.2. Materials

The drilling fluid used in the tests was an ordinary water-based mud provided from one of the southwestern oil fields of Iran. The fluid composition is given in Table 1.

Table 1. Drilling fluid composition.

Drilling Fluid Additives in 350 mL Water	Amount (g)
Soda Ash (Na_2CO_3)	2
NaCl	85
KCl	18
Green Starch	8
Barite	45
Bentonite	10

The additives used in the water-based drilling fluid were selected to provide appropriate rheological behavior, thermal stability, and wellbore pressure control under HPHT conditions. Bentonite was used to improve viscosity and suspension capacity, while Barite was added as a weighting material to control mud density and hydrostatic pressure. Green Starch was incorporated to reduce fluid loss and improve filtration control. In addition, KCl and NaCl were used to enhance shale stability and ionic inhibition, whereas Soda Ash (Na_2CO_3) was added to control water hardness and optimize the chemical conditioning of the drilling fluid.

2.3. Measuring mud weight and rheology

To measure the rheological properties of drilling fluid including plastic viscosity, yield point and gel strengths at different temperatures, a FANN 35SA rotating viscometer equipped with a bath system is used. Also to measure the mud weight at different temperatures, the mud is heated slowly and to make sure that the temperature is set, it is measured by a TP300 thermometer with an accuracy of 0.3°C and then the mud weight is measured using a FANN-TRuWate141 mud balance equipment.

2.4. Test set-up

A set-up device has been designed and constructed based on a narrow-slot model simulating the pipe-tripping operation on a rig. This device can measure the surge and swab pressures, caused by the movement of pipes with different diameters and speeds, in a wide range of temperatures. The schematic of the device is shown in Fig. 1. This device is equipped with a motor with controllable speed as a hoisting system to run the two-part pipe (including a drill pipe of 3 ft length and 1 inch diameter as the upper part and a substitutable drill collar in the lower part with length of 1ft and diameter of 1.5 or 1.75 inch). A centralizing tool limits the pipe movement and prevents any engagements of the inner pipe with the outer pipe (a polyvinylchloride tube with a diameter of 2 inch and length of 5 ft). Five pressure gauges are installed on the outer pipe wall at different heights of 0.164, 0.820, 1.476, 2.133, and 2.789 ft from the datum, measuring pressure changes along the annulus length.

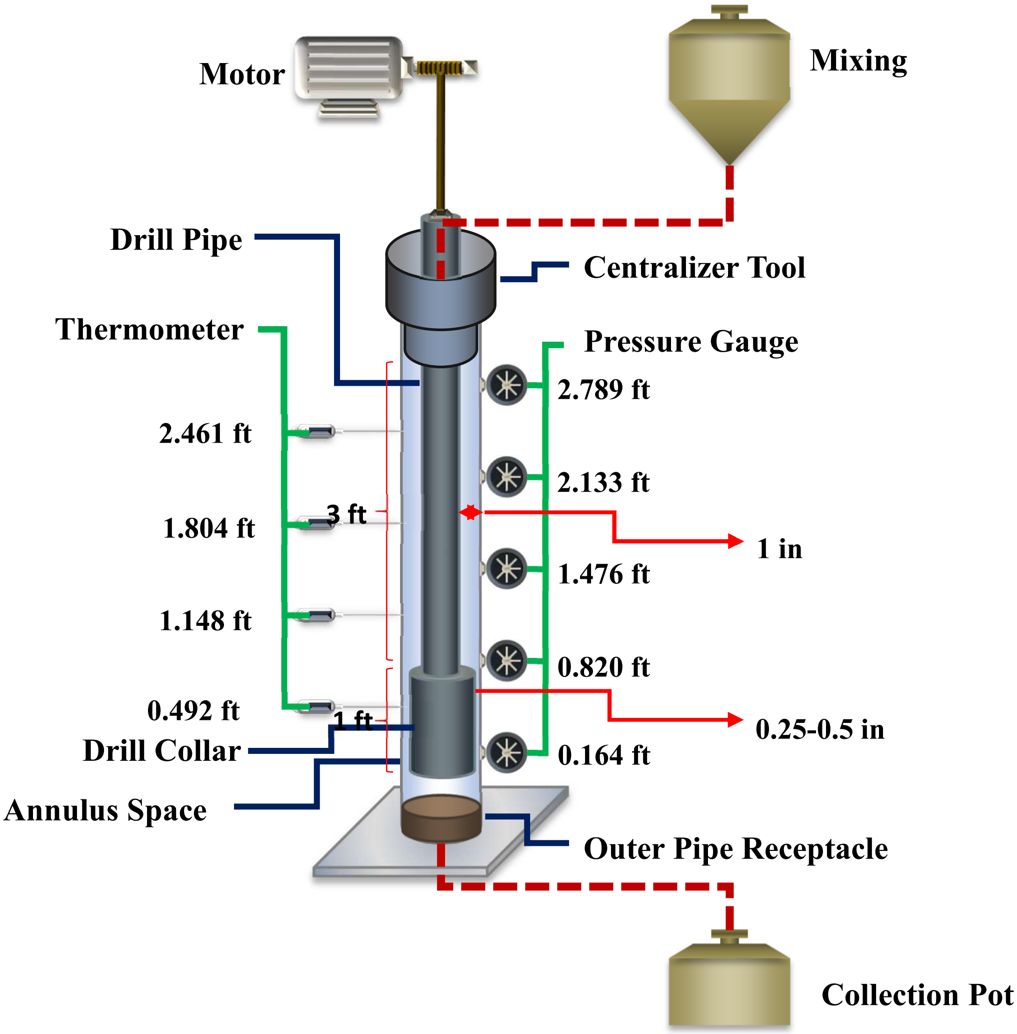

Fig. 1. Schematic of set-up device.

Table 2. Technical specifications and operating conditions of the experimental setup.

Parameter	Specification
Outer pipe inner diameter	2.0 in
Inner pipe diameter	1.0 in
Drill collar diameters	1.5 to 1.75 in
Inner pipe length	3.0 ft
Drill collar length	1.0 ft
Diameter ratio investigated	0.75 and 0.875
Tripping speeds	1.0 and 1.5 ft/s
Pressure sensor configuration	1 main sensor + 4 auxiliary sensors
Pressure sensor elevations	0.164, 0.820, 1.476, 2.133, and 2.789 ft
Main pressure sensor range	0-1000 mbar (≈14.5 psi)
Main pressure sensor accuracy	±1.6% FS
Auxiliary pressure sensor accuracy	±1.0% FS
Temperature sensor configuration	4 sensors along annulus
Temperature sensor accuracy	±0.1°C
Working fluid	Water-based drilling fluid
Flow regime	Predominantly laminar
Data acquisition condition	Steady-state pressure response
Experimental repeats	Each test repeated three times

Four thermometers are installed on the other side of the outer pipe at the heights of 0.492, 1.148, 1.804, and 2.461 ft from the datum to observe the drilling fluid temperature during the tests. A drain valve is installed below the outer pipe so the fluid in the annulus is emptied through it. The main geometrical parameters, operating conditions, and sensor specifications used in the experimental setup are summarized in Table 2.

2.5. Experimental procedure

To establish a reliable experimental procedure, several pilot tests were initially conducted, and the finalized procedure was subsequently adopted for all experiments. First, the drilling fluid was heated gradually while being continuously stirred using a glass rod to ensure uniform temperature distribution and release trapped air bubbles. The prepared mud was then transferred into the outer pipe, and a portion of the fluid was discharged through the lower valve to verify that the drilling fluid properties remained unchanged throughout the preparation stage. The experimental setup was carefully assembled to ensure leak-free operation during all tests. In addition, prior to each experiment, the system was pressurized and allowed to stabilize to confirm the integrity of the sealing conditions and to ensure that no leakage or pressure loss occurred throughout the annular section. For surge pressure measurements, the inner pipe was initially positioned 4 ft above the bottom-hole datum and then tripped downward over a distance of 4 ft at constant velocities of 1 and 1.5 ft/s. The maximum pressure recorded by the lower gauge was considered as the accumulative surge pressure, consisting of hydrostatic and surge pressure components. The pressure differences measured by the gauges installed at different elevations represented the surge pressure response. The experimental data were accepted only when all pressure gauges indicated consistent pressure differentials; otherwise, the test was repeated. For swab pressure measurements, the inner pipe was initially positioned at the bottom-hole datum and then pulled upward over a distance of 4 ft at constant velocities of 1 and 1.5 ft/s. The minimum pressure recorded by the lower gauge was considered as the accumulative swab pressure. Similar to the surge tests, the pressure differentials recorded by the gauges represented the swab pressure response, and only tests with consistent gauge readings were accepted. To ensure repeatability and reliability of the measurements, each experiment was conducted three times and the average values were reported.

3. Modeling Surge and Swab Pressures

To better understand the action mechanisms of different parameters, a mathematical model [3] based on the theory of hydrodynamic viscous drag presented by Maidla and Wojtanowicz [23-25] used was. This model describes the pressure changes due to the movement of a smooth pipe that is placed in the center of a circular close-ended hole (with no wall roughness) filled with an incompressible isothermal one-phase fluid that its rheological properties show a good match with Bingham plastic model. Also, the fluid slippage on the wall is neglected [3].

To calculate the surge and swab pressures, first, the critical pipe velocity must be calculated to determine whether the flow will be laminar or turbulent. As the fluid flows at higher velocities around the pipe with bigger diameters (due to the smaller cross-section around the inner pipe), the calculation must be done for the drill collar [26]. The critical pipe velocity is calculated using Eq. (1) [3]:

$$V_c = \frac{1.08\mu_P + 1.08\sqrt{\mu_P^2 + 9.3\rho(d_H - d_P)^2 Y_P}}{\rho(d_H - d_P)} \tag{1}$$

where V_c is the critical velocity of the pipe (ft/s) and μ_P, Y_P, and ρ stand for plastic viscosity (cP), yield point ($lb_f/100ft^2$), and density of the drilling fluid (lb_m/gal) respectively. Also, d_H and d_P, represent the borehole diameter (inch) and pipe diameter (inch) in order.

In the next step, the annular velocity must be determined around each part of the inner pipe (upper part and lower part) Eq. (2) [3].

In the equation below, V_{ae} is the average annular velocity around the pipe (ft/s), V_p is the pipe velocity (ft/s), δ is the diameter ratio (dimensionless) and C_c is the clinging constant (dimensionless):

$$V_{ae} = V_p \times \left[\frac{\delta^2}{1-\delta^2} + C_c\right] \tag{2}$$

The clinging constant is calculated from the Eq. (3) when the flow around the pipe is laminar, Eq. (3) [3]:

$$C_c = \frac{\delta^2 - 2\delta^2 \ln\delta - 1}{2(1-\delta 2)\ln\delta} = \frac{1}{2\ln\delta} + \frac{\delta^2}{1-\delta^2} \tag{3}$$

When the flow is turbulent in the annulus, the clinging constant is calculated as follows, Eq. (4) [3]:

$$C_c = \frac{\sqrt{\dfrac{\delta^4+\delta}{1+\delta}} - \delta^2}{1-\delta^2} \tag{4}$$

Equation (5) is used to calculate the pressure changes around each pipe while the flow is laminar in the annular space [3]:

$$\Delta P = \frac{L}{300(d_H - d_P)}\left[Y_P + \frac{\mu_P V_{ae}}{5(d_H - d_P)}\right] \tag{5}$$

where ΔP is the pressure change around each pipe (psi) and L is the pipe length (ft).

For turbulent flows around the inner pipe, Eq. (6) is used to calculate the pressure changes due to the pipe movements [3]:

$$\Delta P = \frac{fLV_{ae}^2}{25.8(d_H - d_P)} \tag{6}$$

In Eq. (6), f represents the friction factor (dimensionless) and can be calculated using the Eqs. (7) and (8) [3]:

$$\mathrm{Re} = \frac{926.4 \times \rho V_{ae}(d_H - d_P)}{\mu_P} \tag{7}$$

$$f = e^{\left[c_1 + \frac{c_2}{\mathrm{Re}}\right]} + c_3 \ln(\mathrm{Re}) \tag{8}$$

where Re stands for Reynolds number and c_1, c_2 and c_3 are constants and are given below:

$$c_1 = -3.5378591164$$

$$c_2 = 300.26609292$$

$$c_3 = -0.126153971$$

At the final step, the accumulative surge and swab pressures will be calculated using Eqs. (9) and (10) respectively [3]:

$$P_{acc,surge} = \Delta P_{ap} + \Delta P_{ac} + 0.052\rho h \tag{9}$$

$$P_{acc,swab} = 0.052\rho h - \Delta P_{ap} - \Delta P_{ac} \tag{10}$$

where $P_{acc,surge}$ and $P_{acc,swab}$ denote the accumulative surge and swab pressures (psi), ΔP_{ap} and ΔP_{ac} represent the pressure drops around the drill pipe and drill collar (psi), respectively, and h corresponds to the fluid column height (ft).

The procedure above should be repeated for different pipe diameters running at different velocities in an annulus filled with a fluid with different properties (due to different mud properties at different temperatures).

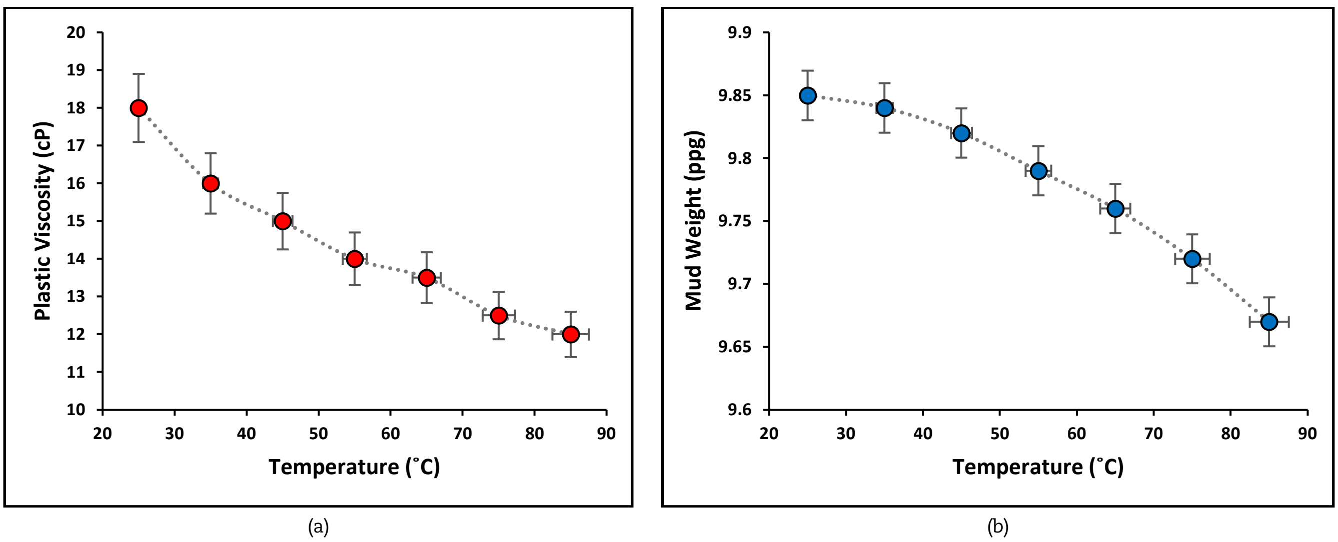

Fig. 2. Mud properties at different temperatures: (a) plastic viscosity, (b) mud weight.

4. Result and Discussion

4.1. Drilling fluid properties

As mud properties are related to its temperature, they were measured at different temperatures using the mentioned equipment in section 2.3 and the results are given in Fig. 2.

As the fluid temperature rises from 25 to 65°C, much of the intermolecular bonds of viscosifier particles break, leading to a great decline in viscosity as can be seen. After that, the rise of temperature from 65 to 85°C (while much of the bonds are broken) would make a slight decrease in viscosity resulting in a total decline of 33% while heating the fluid from 25 to 85°C.

The mud density changes are affected by two parameters while the fluid is heated: the bubbles release [27] and the fluid expansion [28, 29]. The first parameter decreases the effect of the second one to decrease the fluid density. Notably, the bubbles release is a lesser parameter for this fluid and the expansion always prevails.

While heating the fluid, the bubbles exit, and the fluid expands at the same time so the density of the fluid is decreased slightly. After the bubbles are fully released (at around 65°C for this certain drilling fluid) the mud density declines greatly (from 65 to 85°C). The average mud density decrement was observed to be 1.86% according to the figure.

As can be seen in Fig. 3, the shear stress starts with an intercept of 6.0 $lb_f/100ft^2$, and also the shear stress changes at different shear rates almost linearly (the graph changes 97.26% linearly). So, it can be concluded that this drilling fluid behavior can be predicted using the Bingham plastic model. This graph was also plotted for other temperatures as well and the results showed that the fluid behavior is greatly matched with the Bingham plastic model (an average validation of 97% with the Bingham plastic model) [30, 31].

As can be seen in Fig. 3, the shear stress starts with an intercept of 6.0 $lb_f/100\ ft^2$, and also the shear stress changes at different shear rates almost linearly (the graph changes 97.26% linearly). So, it can be concluded that this drilling fluid behavior can be predicted using the Bingham plastic model, which is also in good agreement with the results of previous research [28, 29].

To further evaluate the applicability of the Bingham plastic model under different thermal conditions, the coefficient of determination (R^2) was calculated for all investigated temperatures. The corresponding R^2 values are presented in Table 3. The results indicate a high level of agreement between the experimental rheological data and the Bingham model across the studied temperature range. Although a slight reduction in R^2 is observed with increasing temperature, this trend is attributed to the reduction in drilling fluid viscosity and the progressive weakening of the internal gel structure at elevated temperatures, which leads to minor deviations from the ideal linear shear stress–shear rate relationship assumed in the Bingham model. Nevertheless, all R^2 values remain above 0.95, confirming the robustness and applicability of the Bingham plastic model within the investigated temperature range.

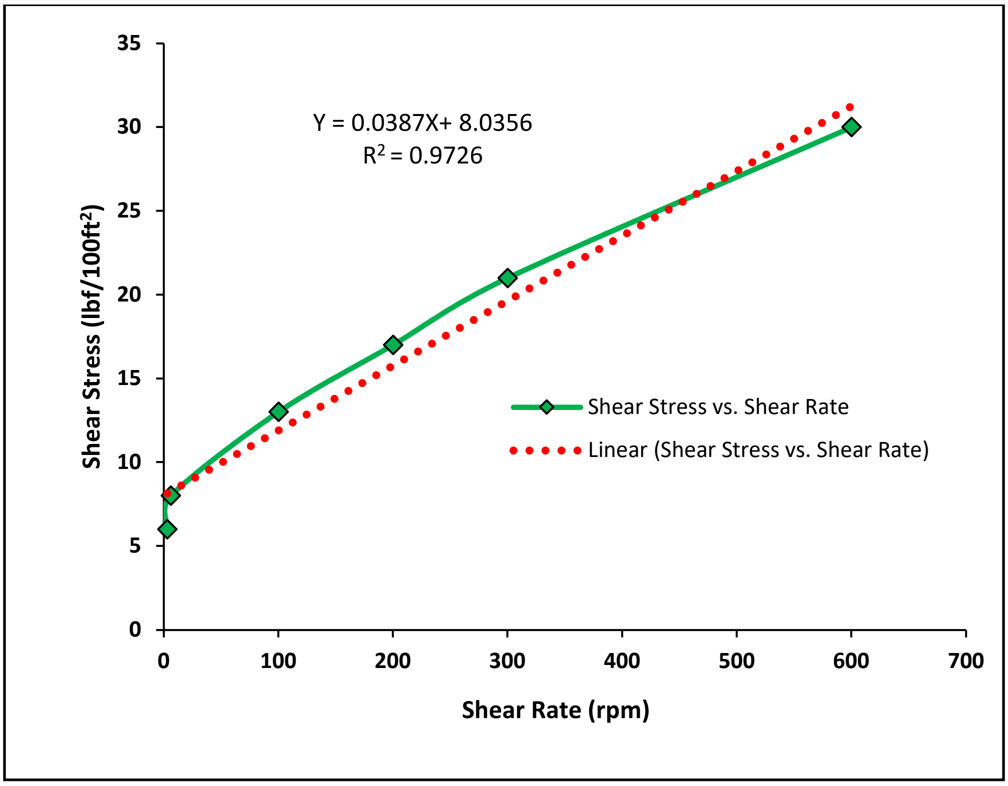

Fig. 3. Drilling fluid shear stress vs. shear rate at 25°C.

Table 3. R^2 of the bingham plastic model at different temperatures.

Temperature (°C)	R^2
25	0.9726
45	0.9689
65	0.9613
85	0.9571

Table 4. Drilling fluid properties.

Temperature (°C)	Mud weight (lb_m/gal)	Plastic viscosity (cP)	Yield point (lb_f/100ft^2)	Gel strength (lb_f/100ft^2)		
				10s	10min	30min
25	9.85	18	52	2.5	3.0	3.0
45	9.82	15	52	2.5	3.0	3.0
65	9.76	13.5	51.5	2.0	2.5	3.0
85	9.67	12	52	2.0	2.0	2.5

To complement the presented analysis of the drilling fluid rheological behavior, a summary of the measured fluid properties, including yield point, plastic viscosity, and gel strength under different experimental conditions, is provided in Table 4.

The reduction in gel strength with increasing temperature can be attributed to the decrease in fluid viscosity, which weakens the intermolecular attractive forces within the drilling fluid system. As temperature increases, the structural network formed by bentonite particles and polymer additives becomes progressively weaker, leading to a less stable gel structure. Consequently, the ability of the drilling fluid to suspend cuttings during static conditions is reduced, and the overall gel network strength diminishes. Although the measured gel strength values fall within a narrow range of approximately 2 to 3 lb_f/100 ft^2, even such small variations are meaningful in transient drilling operations. It should also be noted that the reported values are consistent with the measurement resolution of the FANN 35SA viscometer, typically reported with a step accuracy of 0.5 lb_f/100 ft^2.

From an operational perspective, gel strength plays a critical role in controlling the initial resistance of the drilling fluid to motion during pipe tripping, which directly governs the magnitude of transient pressure responses. During tripping-in operations, a stronger gel structure requires a higher breakout pressure to initiate fluid movement, thereby intensifying the piston effect and leading to higher surge pressures at the bottom hole. This delayed flow response causes a temporary compression of the fluid column in the annulus, increasing pressure transmission to the wellbore. Conversely, during tripping-out operations, a stronger gel structure delays the refill of the annular space, enhancing the suction effect and potentially increasing swab pressure due to incomplete pressure compensation. As temperature increases and gel strength decreases, the drilling fluid exhibits a faster hydraulic response, reducing both the resistance during initial pipe movement and the magnitude of pressure fluctuations. Therefore, temperature-induced variations in gel strength, even within a narrow range, can significantly influence the dynamic balance between hydrostatic support and transient flow resistance, ultimately affecting both surge and swab pressure behavior in HPHT drilling conditions.

4.2. The effect of temperature on surge pressure

At the beginning of the results analysis, it is important to clarify the definition of accumulative pressure used in this study. During tripping operations, the measured accumulative pressure consists of the combined effect of hydrostatic pressure and the transient surge and swab pressures generated by pipe movement inside the annulus. During tripping-in operations, surge pressure acts in the same direction as hydrostatic pressure, resulting in an increase in the accumulative pressure. Conversely, during tripping-out operations, swab pressure acts opposite to hydrostatic pressure, leading to a reduction in the accumulative pressure. Accordingly, the accumulative pressure was calculated as follows:

$$P_{acc,surge} = P_h + P_{surge} \tag{11}$$

$$P_{acc,swab} = P_h - P_{swab} \tag{12}$$

where P_h is the hydrostatic pressure (psi), while P_{surge} and P_{swab} represent the surge and swab pressures (psi), respectively.

The hydrostatic pressure was calculated using:

$$P_h = 0.052 \times \rho \times h \tag{13}$$

It should also be noted that all reported pressures correspond to gauge pressures referenced to atmospheric pressure. The detailed breakdown of hydrostatic, surge, swab, and accumulative pressure data under different experimental conditions is provided in supplementary tables S1 and S2.

The surge phenomena measuring tests were conducted at the constant temperatures of 25, 45, 65, and 85°C and the results are shown in Fig. 4.

As the temperature rises from 25 to 85°C, the surge pressure decreases by 2.8%. Also, as the viscosity of the fluid is greatly decreased from 25 to 65°C (according to Fig. 2), most of the declination in surge pressure occurs in this temperature range. The declination in surge pressure is continuous when rising the temperature from 65 to 85°C due to decrement in drilling fluid density (Although the viscosity of the fluid is decreased only slightly).

4.3. The effect of temperature on swab pressure

To study the effect of temperature on swab pressure, the tests were conducted at 4 different temperatures (25, 45, 65, and 85°C) and the results are given in Fig. 5.

As a result, the reduction in swab pressure becomes the dominant effect, causing the accumulative pressure to increase by approximately 2.86%.

However, when the temperature further increases from 65 to 85°C, the reduction in drilling fluid density becomes more significant. Since hydrostatic pressure is directly proportional to mud density, this density reduction causes a considerable decline in hydrostatic pressure.

Although the swab pressure also continues to decrease due to the lower viscosity, its magnitude becomes relatively small in this temperature range and can no longer compensate for the hydrostatic pressure loss. Consequently, the accumulative pressure decreases by approximately 2.77%, resulting in the extreme point observed in the curve. This behavior demonstrates that the accumulative pressure trend is controlled by the competition between viscosity-dominated swab effects and density-dependent hydrostatic pressure effects. The extreme point therefore represents the transition region where the dominant controlling mechanism shifts from swab-pressure reduction to hydrostatic-pressure reduction as temperature increases.

4.4. Surge pressure changes at different pipe velocities

One of the main factors influencing the surge pressure is pipe tripping velocity and its impact was studied by running the pipe at two different speeds (1 and 15 ft/s) and the results are demonstrated in Fig. 6.

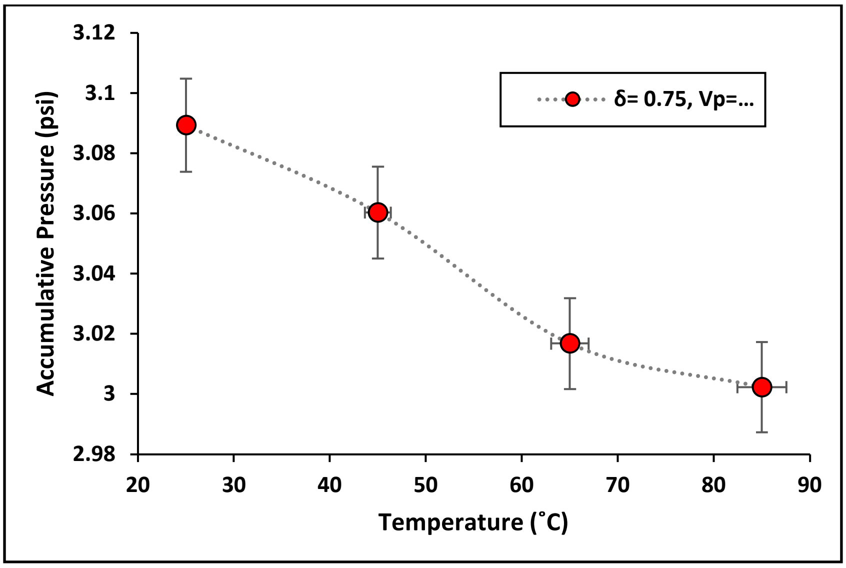

Fig. 4. Accumulative pressure variations during surge phenomena at different temperatures.

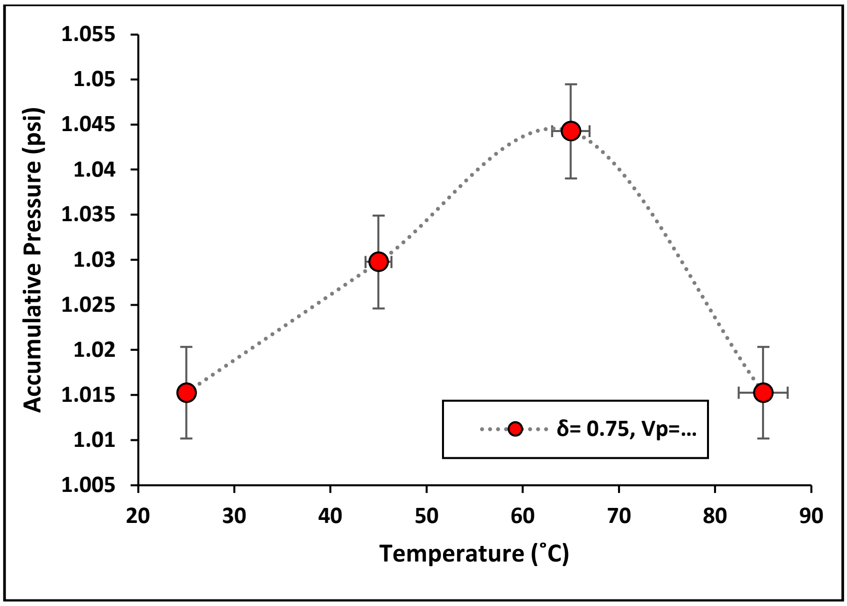

Fig. 5. Accumulative pressure variations during swab phenomena at different temperatures.

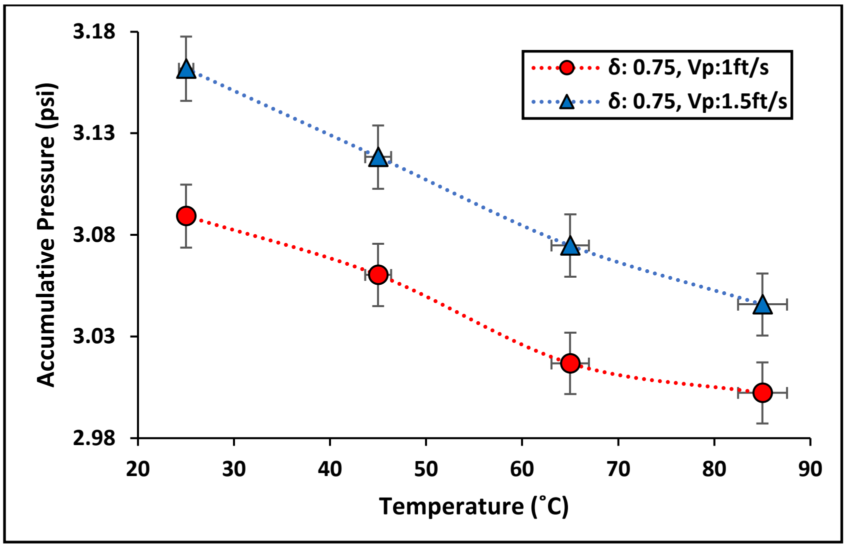

Fig. 6. The effect of pipe velocity on accumulative pressure caused by surging at different temperatures.

As the pipe tripping speed increases, the slippage time of drilling fluid on the pipe wall (both outer and inner pipes) decreases. When the tripping speed is elevated from 1 to 1.5 ft/s, the surge pressure increases by an average amount of 1.9%.

The findings are consistent with the study of Mme and Skalle [3]. It is notable that the viscosity of drilling fluid plays a critical role in the ability of the pipes to carry the fluid in the annulus area so where the viscosity of the mud is higher (from 25 to 65°C for this fluid) the pipe velocity acts more effectively rather than for the mud at lower viscosities (from 65 to 85°C).

4.5. Swab pressure changes at different pipe velocities

The swab pressure is likely to be under the effect of the pipe-tripping velocity. To investigate the effect of tripping speed on swabbing phenomena, the tests were conducted at tripping speeds of 1 and 1.5 ft/s and the outcomes are as given in Fig. 7.

As can be seen in this figure, an increment in pipe tripping speed from 1 to 1.5 ft/s could cause a declination of 5.65% in accumulative pressure due to less slippage time of the fluid over the pipe's surface. The same results were also expressed by other researchers [2, 6, 14]. It can also be observed that when the temperature is between 25 to 65°C, the tripping velocity is more effective on swabbing phenomena (an average of 7.14% inclination in accumulative pressure) than when the fluid temperature is between 65 to 85°C (an average of 4.28% increment in accumulative pressure). It is may be due to the capacity of the surface of the pipe to carry high viscosity fluids more effectively.

4.6. The impact of drill collar diameter on surge pressure

Conducting tests at two different diameter ratios (0.75 and 0.875) could reveal the impact of this parameter on surge phenomena. The results for both diameters are shown in Fig. 8.

The results show that the surge pressure is likely to increase by 52% when running a 1.75-inch pipe (a diameter ratio of 0.875) instead of a pipe with a 1.5-inch diameter (a diameter ratio of 0.75). It may due to the narrower space between the inner pipe and the outer pipe that limits the fluid movement area causing higher surges in flow. The results are consistent with the works of Crespo et al. [2] and Krishna et al. [12]. Also as seen in the figure, the effect of mud viscosity on surge pressure can be strengthened in narrower spaces. The surge pressure changes due to running a larger pipe is more drastic (60%) while the temperature is low (25 to 65°C) and the fluid viscosity is high rather than for a low viscosity fluid at higher temperatures (the pressure change is 45.6% at temperatures between 65 to 85°C). The same results were observed by Tang et al. [14] and Krishna et al. [13].

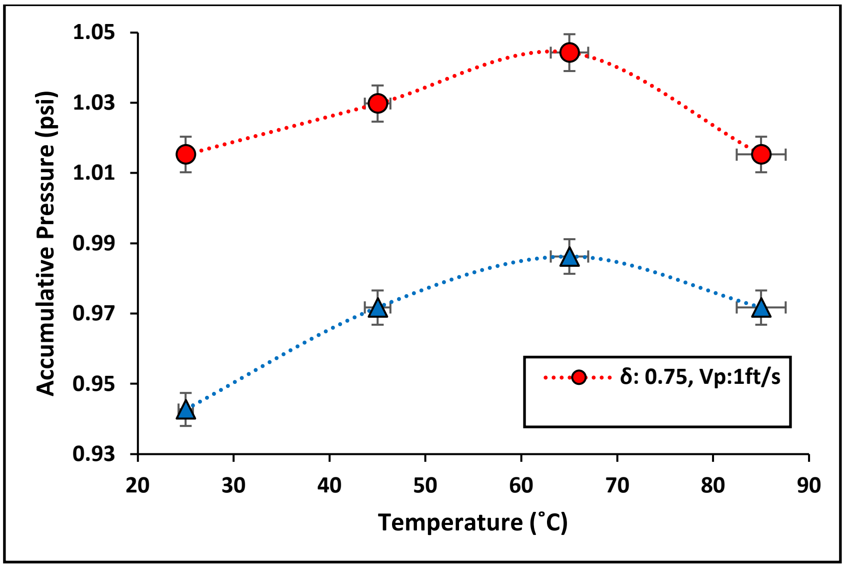

Fig. 7. The effect of pipe velocity on accumulative pressure caused by swabbing at different temperatures.

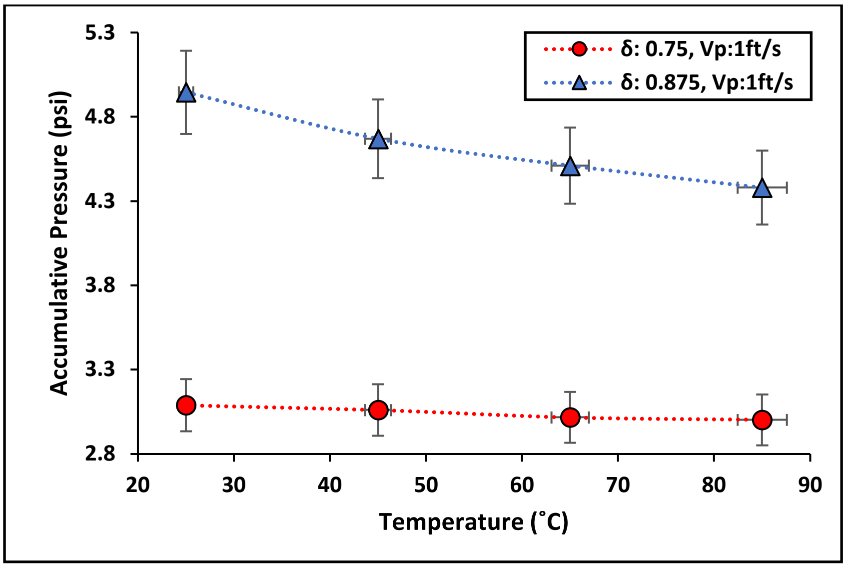

Fig. 8. The effect of diameter ratio on accumulative pressure caused by surging at different temperatures.

4.7. The impact of drill collar diameter on swab pressure

Two different pipe diameter ratios (0.750 and 0.875) were used to investigate the effect of this parameter on swab pressure changes and the test results are shown in Fig. 9. The results indicate that the swab pressure is greatly increased by changing the diameter ratio from 0.75 to 0.875 and the accumulative pressure affected by swabbing at this condition is showing a declination of 62.46% that could be a result of the narrower annular space at higher diameter ratios.

Also, the viscosity changes can be more effective on swab pressure in narrower spaces due to less slippage of the fluid on the pipe surfaces and also the ability of the inner pipe to carry the fluids with higher viscosities (similar to what happens in surge phenomena). This fact can be seen through the difference between swab pressures caused by the two pipes at different temperatures (different temperatures cause different fluid viscosities). It is notable that, at larger diameter ratios, the swabbing phenomena fully prevails over the hydrostatic pressure removing the peak in the accumulative pressure changes diagram.

4.8. Modeling results

To investigate the action mechanisms of different effective parameters on surge and swab pressures, the developed model presented in section 3 was used and the outputs were compared with the experimental results.

Modeling these pressures was done under the same conditions (such as temperature, pipe velocity, and drill collar diameter) that the experimental tests were conducted in. As the maximum pipe tripping speed (1.5 ft/s) did not exceed the minimum critical pipe velocity (minimum critical pipe velocity is calculated from Eq. (1) and it was 9.05 ft/s at different test conditions), the flow was laminar and related equations (Eq. (2), Eq. (3), Eq. (5) and Eq. (9)) were used to predict surge pressure changes. The results are shown in Fig. 10. As can be seen, when the surge phenomenon occurs, the modeling outputs slightly underpredict the experimental results of accumulative pressure changes. The prediction deviation from the experimental data is approximately 3% for a pipe velocity of 1 ft/s and a diameter ratio of 0.75. Increasing the pipe velocity to 1.5 ft/s reduces the prediction accuracy, resulting in an error of approximately 7%. Moreover, increasing the diameter ratio from 0.75 to 0.875 further increases the prediction error to nearly 10%. Although the developed model demonstrates good agreement with the experimental results, these discrepancies mainly originate from simplifying assumptions employed in the modeling procedure and unavoidable experimental uncertainties.

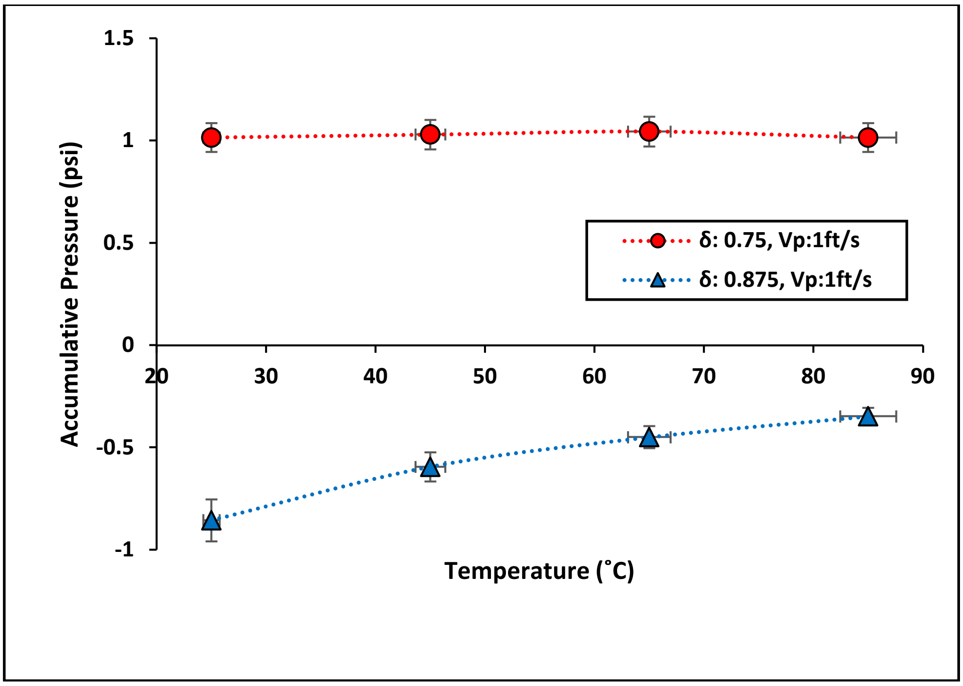

Fig. 9. The effect of diameter ratio on accumulative pressure caused by swabbing at different temperatures.

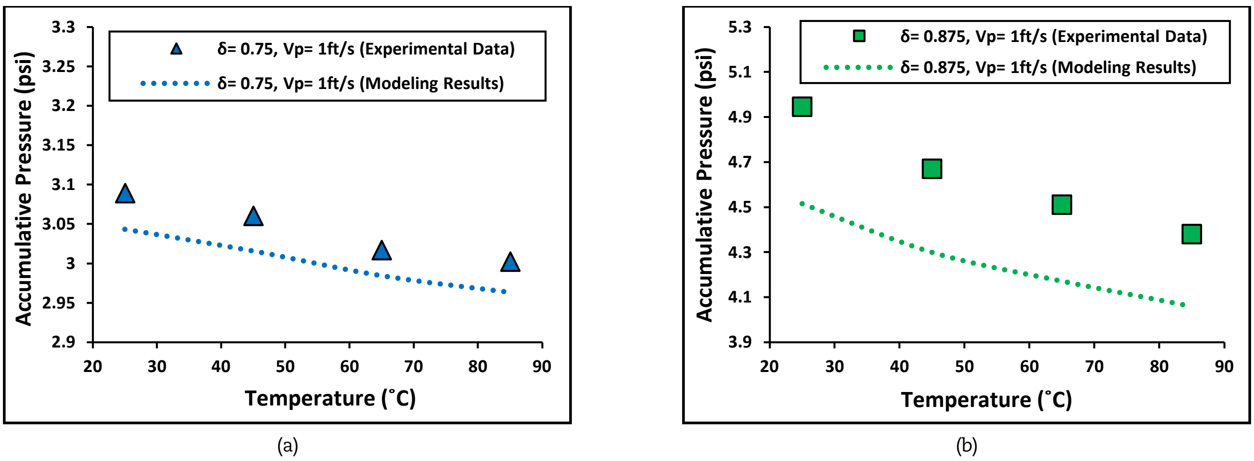

Fig. 10. Modeling results of accumulative surge pressure: (a) V_p = 1 ft/s and δ = 0.75, (b) V_p = 1ft/s and δ = 0.875, (c) V_p = 1.5ft/s and δ = 0.75.

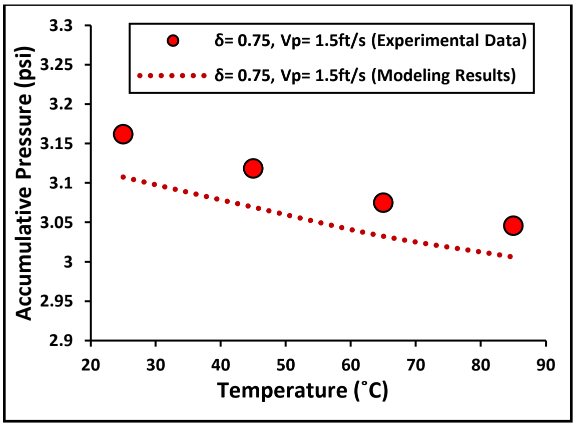

(c)

Fig. 10. Continued.

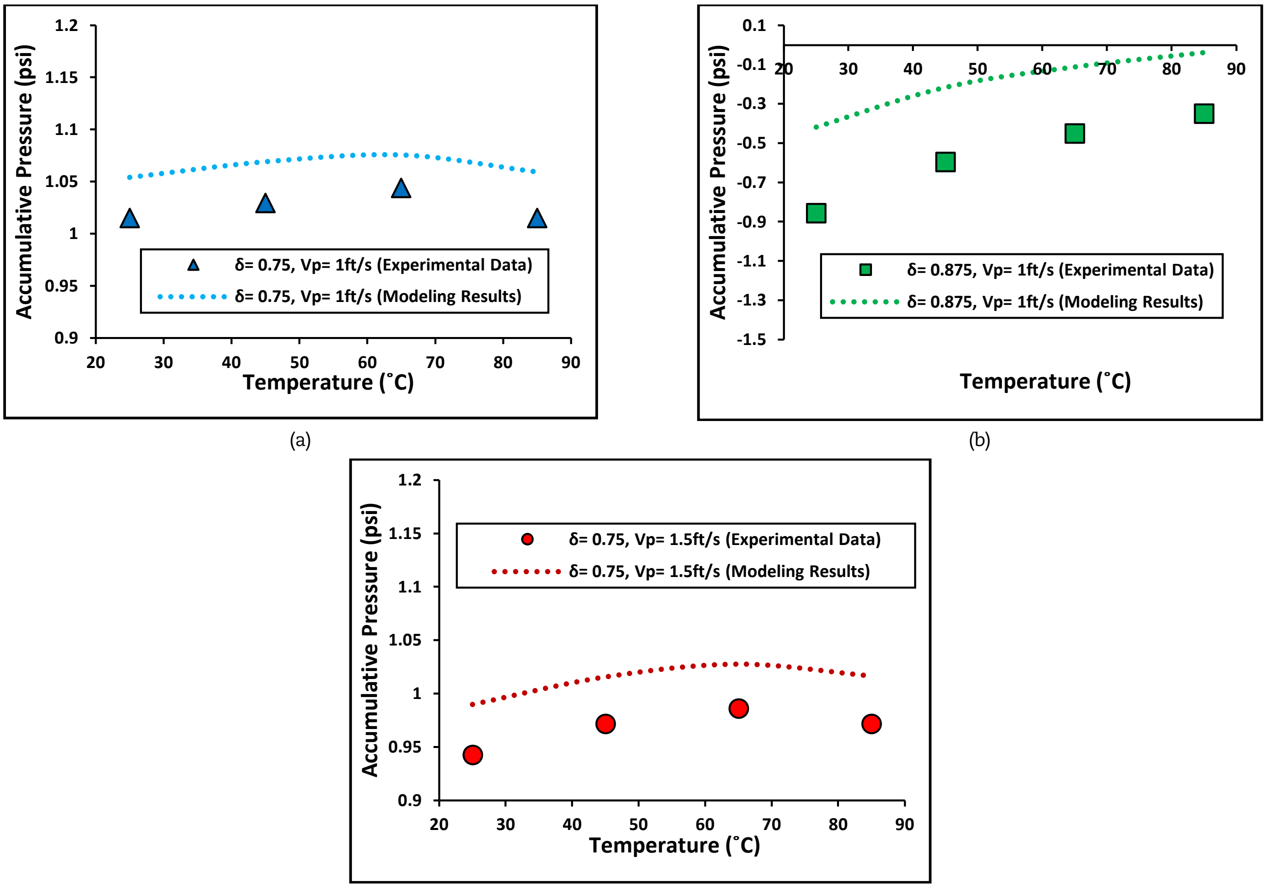

(a) (b)

(c)

Fig. 11. Modeling results of accumulative swab pressure: (a) V_p = 1ft/s and δ = 0.75, (b) V_p = 1ft/s and δ = 0.875, (c) V_p = 1.5ft/s and δ = 0.75.

One important source of deviation is the assumption of hydraulically smooth pipe walls in the model. In the experimental setup, however, the roughness of the drill collar and annular surfaces can locally disturb the velocity profile and generate additional frictional losses, leading to stronger pressure fluctuations than those predicted by the model. This effect becomes more significant at larger diameter ratios because the narrower annular clearance increases wall shear stress sensitivity and intensifies the influence of surface roughness on fluid motion. In addition, despite the overall laminar flow condition, localized transient disturbances may still develop near the moving drill collar even under predominantly laminar flow conditions, particularly at higher tripping velocities. These localized flow instabilities increase momentum transfer and pressure loss, which are not fully captured by the analytical model. Consequently, the developed model tends to slightly underpredict surge pressure at higher pipe velocities.

Comparing the experimental and modeling results also indicates that the swab pressure is slightly underpredicted, leading to a natural overprediction of accumulative pressure during swabbing conditions, unlike the surge-pressure case (Fig. 11).

The modeling error is approximately 1.5% for a pipe velocity of 1 ft/s and a diameter ratio of 0.75. Increasing the tripping speed to 1.5 ft/s slightly increases the prediction error to nearly 2.5%. Furthermore, increasing the diameter ratio to 0.875 raises the prediction error to approximately 7.5%. Another contributing factor to these discrepancies is the assumption of uniform drilling fluid properties throughout the annulus. In practice, localized temperature variations during experiments may slightly affect drilling fluid viscosity and density, thereby influencing surge and swab pressure responses.

Table 5. Extended simulation results of pressure components for different diameter ratios and tripping speeds at 25°C.

Diameter ratio	Tripping speed (ft/s)	Accumulative surge pressure (psi)	Accumulative swab pressure (psi)
0.625	0.5	2.120	1.183
0.625	1.0	2.190	1.123
0.625	1.5	2.270	1.059
0.625	2.0	2.330	0.992
0.750	0.5	2.980	1.110
0.750	1.0	3.044	1.054
0.750	1.5	3.108	0.990
0.750	2.0	3.182	0.920
0.875	0.5	4.180	0.180
0.875	1.0	4.515	-0.418
0.875	1.5	5.142	-1.044
0.875	2.0	5.420	-1.620
0.930	0.5	4.350	-0.051
0.930	1.0	4.780	-0.680
0.930	1.5	5.340	-1.319
0.930	2.0	5.720	-1.948

Furthermore, uncertainties associated with pressure sensor calibration, measurement resolution, and transient sensor response time may also contribute to the observed low-range deviations. Nevertheless, the relatively small prediction errors demonstrate that the developed model is capable of reliably predicting surge and swab pressure behavior under the investigated operating conditions.

To further strengthen the reliability and generality of the observed trends, the modeling results were extended to a wider range of operating conditions. In addition to the experimentally investigated cases, supplementary simulations were performed at a representative temperature of 25°C to evaluate the sensitivity of surge, swab, and accumulative pressures to variations in pipe tripping speed and diameter ratio. This extension was introduced to address the limited number of experimental gradients and to provide a more comprehensive comparison between the governing parameters. The selected range of diameter ratios (0.625–0.93) and tripping speeds (0.5–2.0 ft/s) ensures a physically realistic representation of annular flow conditions while maintaining consistency with the experimental setup. The results obtained from the extended dataset confirm the same overall trend observed experimentally, indicating that the influence of diameter ratio on transient pressure behavior is more pronounced than that of tripping speed. Accordingly, the detailed simulation results are summarized in Table 5 to support the robustness of the model predictions and the validity of the conclusions.

5. Conclusion

To measure the surge and swab pressures a set-up device was designed and constructed simulating a wellbore that a drill string is tripped in/out inside it. Also to better recognize the action mechanism of different parameters' influence on surge and swab pressures, a mathematical model (developed by Mme and Skalle) based on the theory of hydrodynamic viscous drags (by Maidla and Wojtanowicz) was used and the results showed that:

- Increasing the fluid temperature from 25 to 85°C leads to lower viscosity and density of the fluid which leads to lower surge and swab pressures.
- Pipe diameter ratio, tripping velocity, mud viscosity, and mud density have a significant effect on surge and swab pressure.
- For the swab phenomenon, as the fluid temperature rises, the accumulative pressure first increases due to weaker swabbing (due to lower viscosity of the fluid at higher temperatures) and then decreases as a result of hydrostatic pressure declination (due to lower mud density at higher temperatures).
- For the surge phenomenon, as the temperature rises, the accumulative pressure is reduced drastically due to a decrement in surge pressure (as a result of lower fluid viscosity at higher temperatures), and the hydrostatic pressure declination (as the temperature rises, the mud density is decreased).
- The modeling results show an acceptable validation of 97% for surge and swab pressure predictions.
- An increment in diameter ratio (from 0.75 to 0.875) and tripping velocity (from 1 to 1.5 ft/s) could decrease the modeling validation to 90% and 94% respectively.

The findings of this study can serve as a useful foundation for further investigations into surge and swab pressure behavior under more complex and extreme operational conditions. In particular, the presented results provide a basis for extending the analysis to higher temperature ranges, broader geometric configurations, and more diverse drilling fluid systems. Such future developments can contribute to a more comprehensive understanding of the governing mechanisms of transient pressure behavior and improve the predictive capability of numerical models and drilling simulators. Ultimately, this line of research may support more accurate risk assessment and better operational decision-making in drilling engineering applications.

Author Contributions

M. Mombeini conducted the investigation, performed the formal analysis, developed the mathematical modeling, and prepared the original draft of the manuscript. M. Torkaman contributed to the formal analysis and methodology, reviewed and edited the manuscript, and supervised the research process. M. Mohammareh Nezhad Rabieh provided the necessary resources and participated in the supervision of the study. M. Moradi was responsible for the conceptualization of the research and data curation.

Acknowledgments

The authors appreciated the financial support from Shahid Chamran University of Ahvaz (Grant No.: SCU.EC1401.44294).

Conflict of Interest

The authors declare that there is no conflict of interest.

Funding

The authors received no financial support for the research, authorship, and publication of this article.

Data Availability Statements

The datasets generated and/or analyzed during the current study are available from the corresponding author on reasonable request.

Nomenclature

V_c	Critical velocity of the pipe [ft/s]	BHP	Bottom-hole pressure
V_{ae}	Average annular velocity around the pipe [ft/s]	HPHT	High pressure–high temperature
C_c	Clinging constant (dimensionless)	NS	Narrow-slot
L	Pipe length [ft]	BHP	Bottom-hole pressure
F	Friction factor (dimensionless)	HPHT	High pressure–high temperature
Re	Reynolds number	NS	Narrow-slot
P_{surge}	Surge pressure [psi]	PAM	Polyacrylamide
P_{swab}	Swab pressure [psi]	XG	Xanthan gum
d_H	Borehole diameter [inch]	ANN	Artificial neural network
d_P	Pipe diameter [inch]	LSTM	Long short-term memory
Y_P	Yield point [lbf/100ft^2]	NPT	Non-productive time
h	Height [ft]	MPD	Managed pressure drilling
P_h	Hydrostatic pressure [psi]	FS	Full scale
R2	Coefficient of determination	BHA	Bottom hole assembly
ΔP	Pressure changes around each pipe [psi]	δ	Diameter ratio (dimensionless)
$P_{acc,surge}$	Accumulative surge pressure [psi]	μ_P	Plastic viscosity [cP]
$P_{acc,swab}$	Accumulative swab pressure [psi]	ac	Around drill collar
ap	Around pipe	H	Hole
P	Pipe	ρ	Fluid density [lbm/gal]

References

[1] Payne, M.L., Pattillo, P.D., Miller, R.A., Johnson, C.K., Advanced technology solutions for next generation HPHT wells, International Petroleum Technology Conference, Dubai, U.A.E., Paper No. IPTC-11463-MS, 2007.
[2] Crespo, F., Ahmed, R., Enfis, M., Saasen, A., Amani, M., Surge-and-swab pressure predictions for yield-power-law drilling fluids, *SPE Drilling & Completion*, 27, 2012, 574-585.
[3] Mme, U., Skalle, P., Effects of mud properties, hole size, drill string tripping speed and configurations on swab and surge pressure magnitude during drilling operations, *International Journal of Petroleum Science and Technology*, 2012, 143-153.
[4] Crespo, F., Ahmed, R., A simplified surge and swab pressure model for yield power law fluids, *Journal of Petroleum Science and Engineering*, 101, 2013, 12-20.
[5] Srivastav, R., Enfis, M., Crespo, F., Ahmed, R., Saasen, A., Laget, M., Surge and swab pressures in horizontal and inclined wells, SPE Latin America and Caribbean Petroleum Engineering Conference, Mexico City, Mexico, Paper No. SPE-152662-MS, 2012.
[6] Tang, M., Xiong, J., He, S., A new model for computing surge/swab pressure in horizontal wells and analysis of influencing factors, *Journal of Natural Gas Science and Engineering*, 19, 2014, 337-343.
[7] Al-Abduljabbar, A.M., Hossain, M.E., Gharbi, S., Al-Rubaii, M.M., Optimization of tripping speed to minimize surge & swab pressure, SPE/IADC Middle East Drilling Technology Conference and Exhibition, Abu Dhabi, UAE, 2018.
[8] He, S., Srivastav, R., Tang, M., Ahmed, R., A new simplified surge and swab pressure model for yield-power-law drilling fluids, *Journal of Natural Gas Science and Engineering*, 28, 2016, 184-192.
[9] Wang, X., Peng, F., Zhang, F., Sheng, C., Xiang, J., Lou, W., A temperature-and pressure-coupled model for surge pressure in high-temperature, high-pressure wells, *SPE Journal*, 31, 2026, 876-890.
[10] Li, Y. et al., Transient surge/swab pressure modeling and tripping velocity optimization in managed pressure drilling with a choke-controlled outlet, *SPE Journal*, 2026, 1-24.
[11] Krishna, S., Ridha, S., Vasant, P., Ilyas, S.U., New analytical approach for predicting surge/swab pressure gradient using mud clinging effect and frictional pressure losses: For yield power law fluid, Offshore Technology Conference Asia, Kuala Lumpur, Malaysia, Paper No. D012S001R028, 2020.
[12] Krishna, S., Ridha, S., Vasant, P., Ilyas, S.U., Irawan, S., Gholami, R., Explicit flow velocity modelling of yield power-law fluid in concentric annulus to predict surge and swab pressure gradient for petroleum drilling applications, *Journal of Petroleum Science and Engineering*, 195, 2020, 107743.

[13] Krishna, S., Ridha, S., Campbell, S., Ilyas, S.U., Dzulkarnain, I., Abdurrahman, M., Experimental evaluation of surge/swab pressure in varying annular eccentricities using non-Newtonian fluid under Couette-Poiseuille flow for drilling applications, *Journal of Petroleum Science and Engineering*, 206, 2021, 108982.
[14] He, S., Tang, M., Wang, W., Xiong, J., Numerical model for predicting the surge and swab pressures for yield-power-law fluids in an eccentric annulus, *Journal of Natural Gas Science and Engineering*, 26, 2015, 28-34.
[15] Tang, M., Zhang, T., He, S., Kong, L., Li, H., Li, Q., Modeling of laminar flow in an eccentric elliptical annulus for YPL fluid, *Journal of Natural Gas Science and Engineering*, 64, 2019, 118-132.
[16] Mohammad, A., Belayneh, M., New simple analytical surge/swab pressure model for power-law and modified yield-power-law fluid in concentric/eccentric geometry, *Applied Sciences*, 13, 2023, 12867.
[17] Mohammad, A., Belayneh, M., Davidrajuh, R., Physics-based swab and surge simulations and the machine learning modeling of field telemetry swab datasets, *Applied Sciences*, 13, 2023, 10252.
[18] Yusuf, M., Ridha, S., Krishna, S., Sabo, U.N., Prediction of surge/swab pressure in the oil & gas industry: Effect of process parameters and significance of modeling, in Advances in Material Science and Engineering, Springer Nature Singapore, 2024.
[19] Zhang, Z., Xiang, S., Liu, S., Luo, M., Jiang, W., Study on the influence of tripping operation on annular transient surge-swab pressure of Herschel–Bulkley fluid, *Journal of Energy Resources Technology*, 145, 2022, 1-23.
[20] Salih, F., Hadi, F., Estimation of surge and swab pressures while tripping for minimizing excessive drilling problems, *Iraqi Geological Journal*, 57, 2024, 174-200.
[21] Kamgue Lenwoue, A.R., Li, Z., Hu, P., Songwe Selabi, N.B., Wandji Djouonkep, L.D., Effect of swab and surge pressure on the time-dependent wellbore natural fracture development, *Geomechanics and Geophysics for Geo-Energy and Geo-Resources*, 10, 2024, 107.
[22] Wei, K., Xiao, D., Xi, C., Wu, D., Liao, H., Numerical simulation and analysis of holebottom pressure fluctuations during tripping operations in deep and complex wells, *Physics of Fluids*, 37, 2025.
[23] Maidla, E.E., Wojtanowicz, A.K., Field comparison of 2-D and 3-D methods for the borehole friction evaluation in directional wells, SPE Annual Technical Conference and Exhibition, Dallas, USA, Paper No. SPE-16663-MS, 1987.
[24] Maidla, E.E., Wojtanowicz, A.K., A field method for assessing borehole friction for directional well casing, *Journal of Petroleum Science and Engineering*, 1, 1988, 323-333.
[25] Maidla, E.E., Wojtanowicz, A.K., Laboratory study of borehole friction factor with a dynamic-filtration apparatus, *SPE Drilling Engineering*, 5, 1990, 247-255.
[26] Eckhardt, B., Schneider, T.M., Hof, B., Westerweel, J., Turbulence transition in pipe flow, *Annual Review of Fluid Mechanics*, 39, 2007, 447-468.
[27] Gonnermann, H.M., Manga, M., The fluid mechanics inside a volcano, *Annual Review of Fluid Mechanics*, 39, 2007, 321-356.
[28] App, J.F., Field cases: Nonisothermal behavior due to Joule-Thomson and transient fluid expansion/compression effects, SPE Annual Technical Conference and Exhibition, New Orleans, USA, Paper No. SPE-124338-MS, 2009.
[29] Patterson, M.J., Stocks, J.M., Taylor, N.A.S., Sustained and generalized extracellular fluid expansion following heat acclimation, *The Journal of Physiology*, 559, 2004, 327-334.
[30] Lipscomb, G., Denn, M., Flow of Bingham fluids in complex geometries, *Journal of Non-Newtonian Fluid Mechanics*, 14, 1984, 337-346.
[31] Kent, J.T., The Fisher-Bingham distribution on the sphere, *Journal of the Royal Statistical Society: Series B (Methodological)*, 44, 1982, 71-80.

ORCID iD

Mohammad Torkaman https://orcid.org/0000-0001-6329-864X

How to cite this article: Mombeini M. et al., Experimental and Modeling Approach to Investigate the Influence of Temperature on Surge and Swab Pressures in Water-Based Drilling Muds, *J. Appl. Comput. Mech.*, xx(x), 2026, 1–14. https://doi.org/10.22055/jacm.2026.48857.5554